Research Square

Preprints are preliminary reports that have not undergone peer review.
They should not be considered conclusive, used to inform clinical practice,
or referenced by the media as validated information.

Callus Culture System from Lonicera japonica Thunb Anthers : Light Quality Effects on Callus Quality Evaluation

Jiali Cheng
Gansu Agricultural University
Fengxia Guo
Gansu Agricultural University
Chunyan Zhou
Hexi University
Yong Chen
Xinjiang Academy of Agricultural Sciences
Zhigang Li
Longxi County Agricultural Technology Extension Center
Wei Liang
Gansu Agricultural University
Hongyan Wang
Gansu Agricultural University
Yuan Chen
chenyuan@gsau.edu.cn
Gansu Agricultural University
Pengbin Dong
Gansu Agricultural University

Research Article

Keywords: L. japonica, Callus culture, Light quality, Histomorphological structure, Bioactive metabolite

Posted Date: October 4th, 2024

DOI: https://doi.org/10.21203/rs.3.rs-5016954/v1

License: This work is licensed under a Creative Commons Attribution 4.0 International License. Read Full License

Additional Declarations: No competing interests reported.

Abstract

Lonicera japonica Thunb has significant edible and medicinal value, offering properties like heat clearing, detoxification, antibacterial, and blood pressure reduction. However, its quality is limited by climate, environment, flowering period, and germplasm degradation. This study established the first embryogenic callus culture system for *L. japonica* anthers. Using abiotic inducers (light quality), the effects on callus morphology, metabolite accumulation, and antioxidant activity were examined. Results showed that adding 1.0 mg·L^{-1} 6-BA, 1.5 mg·L^{-1} NAA, 1.5 mg·L^{-1} 2,4-D, and 0.2 mg·L^{-1} KT to MS medium induced 81% embryogenic callus. Subculturing with 2.0 mg·L^{-1} 6-BA, 0.5 mg·L^{-1} NAA, and 0.2 mg·L^{-1} KT yielded uniform callus lines. SEM and paraffin sectioning distinguished callus types. After 15 days of blue light induction, active metabolites and antioxidant activities peaked. This system supports germplasm innovation and suggests abiotic inducers as a method for higher metabolic product yields.

1 Introduction

Lonicerae japonicae flos is the dried flower buds of *Lonicera japonica* Thunb, which is also known as Jin Yin Hua and Japanese honeysuckle[1]. It is a member of the Caprifoliaceae family and is highly regarded as a traditional herb in East Asia[2]. With a history spanning millennia, *L. japonica* stands as a cornerstone of Traditional Chinese Medicine, renowned for its multifaceted therapeutic attributes including antibacterial, anti-inflammatory, antioxidant, antiviral, and anticancer properties[3,4,5,6,7]. Its pharmacological activities primarily stem from secondary metabolites, including organic acids, flavonoids, iridoids, saponins, etc[2,8,9]. For instance, phenolic compounds play significant roles in anti-inflammatory, anti-aging, and antioxidant activities, while flavonoids exhibit positive effects in treating chronic diseases such as coronary heart disease, cancer, and diabetes[10,11]. Furthermore, it has also been used as a dietary supplement, tea, and beverage, referred to as “Functional Food”[12].

According to “The Statistics from the National Economic Forest Association,” the global market demand for *L. japonica* has exceeded 20 million kilograms, yielding an output value of up to USD 860 million, making it one of the most economically valuable medicinal herbs[13]. However, due to limited land resources, large-scale cultivation is unsustainable[14]. Furthermore, the quality and yield of medicinal substances have been constrained by the lack of cultivated variations over extended cultivation periods[15]. Additionally, plants grown in field conditions as sources of secondary metabolites are subject to constraints imposed by geographical, seasonal, and climatic factors[16]. Moreover, further extraction and purification of secondary metabolites from intact plants is a complex and time-consuming process; furthermore, the bioactivity of compounds is comparatively low[17]. Consequently, plant tissue culture is considered an avenue for optimizing the production of secondary metabolites, ensuring their stability against external environmental fluctuations and guaranteeing a sustainable supply of active compounds. In summary, plant cell culture provides an attractive platform for the large-scale production of plant chemical constituents and lays the groundwork for germplasm innovation in medicinal resources

Predecessors have employed various strategies to augment metabolite productivity in in vitro cultures[18]. Elicitation has been reported as one of the most effective strategies for increasing secondary metabolite synthesis in plant cell culture[19,20]. Among biological and non-biological elicitors, light stands out as a significant non-biological factor, playing a crucial regulatory role in the developmental patterns of in vitro cultured tissues and promoting the production of secondary metabolites[21]. Previous studies have confirmed the stimulatory effect of light on the accumulation of secondary metabolites. For example, in callus cultures of *Stevia rebaudiana*, there were improvements observed in total phenolics, total flavonoids, and total antioxidant capacity[22]. Significant alterations in both morphological and biochemical attributes were observed in mature leaf callus cultures of *Artemisia absinthium L.*[21]. Similarly, biomass accumulation and the production of antioxidant secondary metabolites were significantly enhanced in callus cultures of

Prunella vulgaris[23]. Moreover, changes were observed in the morphological growth, accumulation of phenolic compounds, and total antioxidant capacity of red callus cultures of *Vitis vinifera*[24].

Callus tissues can be induced from different explants, and the characteristics of callus tissues vary depending on their origins. For example, in *Cnidium officinale*, root explants exhibit the highest formation rate of callus tissues compared to stem explants[25]. In *Centella asiatica (L.)*, triterpenoid secondary metabolites are abundantly present in roots induced from leaf explants[26]. When callus tissues induced from leaves, stems, and roots of *Hypericum triquetrifolium Turra* were treated with gamma irradiation, it was found that the content of p-OH-benzoic acid was higher in callus tissues induced from leaf explants, while the highest content of chlorogenic acid was observed in callus tissues induced from root explants[27]. In *Lycium barbarum L.*, among different explants (leaf, petiole, root, hypocotyl, and node), hypocotyl explants yielded the largest diameter of callus tissues[28]. Anthers of black rice can produce light yellow and spherical sporogenous callus tissues[29]. While callus induction from various explants of *L. japonica* has been reported in previous studies[14], callus induction from anther explants of *L. japonica* has not been reported.

This study utilized the anthers of *L. japonica* as the source material and established a method for inducing callus tissues from *L. japonica* anthers, resulting in the acquisition of high-quality callus tissue materials. Morphological and cytological observations were conducted on the callus tissues, revealing both common and unique characteristics. Additionally, significant emphasis was placed on employing elicitor-mediated methods to analyze the growth of callus tissues, synthesis of secondary metabolites, and gene expression in *L. japonica* callus tissues. The establishment of a callus tissue system derived from *L. japonica* anther culture lays the foundation for the rapid production of purebred plants and the improvement of *L. japonica* germplasm resources. Elicitor-mediated techniques contribute to enhancing the accumulation of secondary metabolites, improving the quality of medicinal plants, and opening new avenues for pharmaceutical development.

2 Material and methods

2.1 Experiment Materials

Different-sized flower buds of *L. japonica* were harvested from the Tongwei Qingliangyuan Company base and authenticated by Professor Yuan Chen (Gansu Agricultural University, Lanzhou, China). The harvested materials were placed in self-sealing bags and stored at 4°C for 24 h. They were thoroughly washed in running tap water for 30 minutes, followed by immersion in a 75% ethanol solution for 30 seconds in a laminar flow hood. Afterward, they were rinsed 3–5 times with sterile water and then soaked in a 0.1% mercuric chloride solution for 8–10 minutes before being rinsed again with sterile water 3–5 times.

2.2 Association between flower bud/floret size and developmental stage of microspores

Measure the length of the flower buds and fix them at room temperature in Carnoy's solution (100% ethanol and glacial acetic acid, 3:1) for 24 hours, followed by ethanol gradient elution. To establish the correlation between bud size and microspore developmental stages, select 6 buds from each size category: 0.5–0.7 cm, 1.0-1.4 cm, 1.8-2.0 cm, 2.3–2.6 cm, 2.8–3.2 cm, and 3.5–3.8 cm. Dissect the anthers from the buds, and gently squeeze them with tweezers to release the contents. Add 1–2 drops of acetocarmine solution and leave in a dark environment for 30 minutes. Observe under an optical microscope. Then, add 1 drop of 4',6-Diamidino-2-phenylindole (DAPI) staining solution and observe under a fluorescence microscope (RVL-100-G, ECHO, CA, United States).

2.3 Callus induction

Disinfected flower buds were decapitated, and the petals were removed. The anthers were then inoculated into culture bottles containing 50 mL of solid medium supplemented with various concentrations of plant growth regulators (PGRs). Each treatment was replicated 10 times. The basal medium consisted of solid Murashige & Skoog (MS) medium, 0.5% (w/v) agar, and 3% (w/v) sucrose. Growth regulators, including naphthalene acetic acid (NAA), 2,4-dichlorophenoxy acetic acid (2,4-D), kinetin (KT), and 6-benzyladenine (6-BA), were added to the basal medium to induce callus formation. Based on the results of the single-factor experiment, an L_9 (3^4) orthogonal test was conducted to optimize the concentration levels of PGRs. Detailed information on the L_9 (3^4) orthogonal matrix is provided in Table 2. The medium (pH 5.8) was sterilized by autoclaving at 121°C and 1.01×105 Pa for 25 minutes. All cultures were incubated in a growth chamber at 20 ± 2°C with 75% relative humidity under dark conditions for 7 days, followed by a 45-day photoperiodic culture under a 12-hour dark/12-hour white fluorescent light (60 $\mu molm^{-2} s^{-1}$).

2.4 Callus proliferation

After 52 days of induction, 0.5 g of yellow, fragile callus tissue was transferred onto fresh 50 mL MS medium supplemented with agar, sucrose, and PGRs. The optimization of PGRs concentrations was based on another orthogonal design, L_9 (3^4), with the levels of each factor detailed in Table S1. The pH of the medium was adjusted to 5.8, and as previously described in Section 2.3, the medium was sterilized. All cultures were maintained on shelves in a growth chamber at 20 ± 2°C with 60% relative humidity under a 12-hour dark/12-hour white fluorescent light (60 $\mu molm^{-2} s^{-1}$) photoperiod. Callus proliferation phenomena were observed after 45 days of culture.

2.5 Histomorphological observation of callus

2.5.1 Scanning electron microscopy (SEM)

Following the methodologies outlined by Popielarska-Konieczna et al[30]. and Liu et al[31]., the morphological variations of callus tissues under different treatments were fixed in 3% glutaraldehyde buffer (0.1 M phosphate buffer, pH 7.2) at room temperature for 2 hours. Subsequently, they were subjected to ethanol dehydration at varying concentrations, followed by immersion in tert-butanol at 4°C. The specimens were then dried and mounted on aluminum stubs with conductive adhesive. Gold coating was applied before observation under a scanning electron microscope (S-3400 N Hitachi, Japan) at a voltage of 15 kV.

2.5.2 Paraffin sections

According to previous descriptions, the histological structure of callus tissues was observed[32,33]. In brief, the callus tissues were sequentially fixed in FAA fixative, dehydrated in varying concentrations of ethanol, immersed in a mixture of ethanol and xylene, soaked in a mixture of xylene and paraffin, and embedded in paraffin cubes. The embedded samples were sectioned into 7 μm slices and stained with safranin O fast green FCF. Subsequently, the histological structure of callus tissues was observed using a microscope (RVL-100-G, ECHO, CA, United States).

2.6 Induction of callus proliferation under different light conditions

The 1 g callus was transferred onto growth medium containing the optimal hormone ratio, as determined previously (Section 2.3). As described earlier, the medium was sterilized, and then placed on three separate shelves under 100% blue, 100% red, and 100% white fluorescent light settings, maintaining a 12-hour photoperiod at 20 ± 2°C with 75% relative humidity. Callus were observed after 30 days of culture.

2.7 Phytochemical Analysis

Dry *L. japonica* callus tissue samples were pulverized using a mortar and pestle, and 0.15 g of the sample was weighed and immersed in 50 ml of methanol solution Subsequently, ultrasonic treatment. Then, the extracts were centrifuged at

5000 rpm for 5 minutes at 4°C, and the supernatant was collected and filtered through a 0.22 μm organic filter membrane. The filtered extracts were stored at 4°C until further analysis.

2.7.1 Determination of Total Flavonoid, Total Phenolic and soluble sugar

2.7.1.1 Total Flavonoid Content

The total flavonoid content was determined using the sodium nitrite-aluminum nitrate-sodium hydroxide method[34,35]. Briefly, 600 μl of the extract was added to the reaction mixture, and the absorbance was measured at 510 nm using a UV-Vis spectrophotometer (Genesys 10 S UV-Vis, Thermo Scientific). A standard calibration curve was constructed using catechin (0.2-1.0 mg/ml). Total flavonoid content was expressed as mg CE (catechin-equivalents)/ g DW.

2.7.1.2 Total phenolic Content

The total phenolic content was measured using the Folin-Ciocalteu method[36,37]. Briefly, 600 μL of the extract was added to the reaction mixture, and the absorbance was read at 760 nm using a spectrophotometer. A standard calibration curve was constructed using gallic acid (0.02–0.1 mg/ml). The total phenolic content was expressed as mg GAE (gallic acid equivalents)/ g DW.

2.7.1.3 Soluble sugar Content

Soluble sugar content was measured using the sulfuric acid-phenol method[38]. Briefly, 500 μL of the extract was added to the reaction mixture, and the absorbance was read at 485 nm using a spectrophotometer. A standard calibration curve was prepared using sucrose (0.05–0.6 mg/ml). Soluble sugar content was expressed as mg SSE (Soluble Sugars-equivalents)/ g DW.

2.7.2 Determination of antioxidant capacity

Two widely used methods, namely DPPH and FRAP assays, were employed to assess the in vitro antioxidant capacity[39]. For the DPPH assay, following a previously established protocol[40], 500 μL of the extract was added to the reaction mixture, and the absorbance was measured at 515 nm using a spectrophotometer. For the FRAP assay, following established protocols[41,42], 500 μL of the extract was added to the reaction mixture, and the absorbance was measured at 593 nm using a spectrophotometer. A calibration curve using 500 μM ascorbic acid was used as a reference standard.

2.8 HPLC fingerprint establishment

To establish HPLC fingerprints, the chromatographic conditions were optimized and the established method was verified. 1. Method Establishment : On the HPLC detection platform, which were set as follows: 1) column, Symmetry C18 (5μm, 4.6mm*250mm); 2) mobile phase: acetonitrile (Merck) as mobile phase A, ultrapure water with 0.1% phosphoric acid (Aladdin) as mobile phase B; 3) elution gradient: starting conditions of 9% B, 15 → 17.5% A (from 10.00 to 20.00 min), 17.5 → 17.8% A (from 20.00 to 30.00 min), 17.8 → 22% A (from 30.00 to 40.00 min), 22 → 9% A (from 40.00 to 50.00 min); 4) wavelength, column temperature, flow rate, and injection volume: 245nm, 38℃, 1 ml/min, 10 μL, respectively. 2. Method Validation: Evaluate precision by injecting the same sample solution six times in a row, and assess repeatability by analyzing six different sample solutions prepared in parallel with the same procedure and batch of *L. japonica.* Stability tests of the sample solutions are conducted by analyzing them at 0, 2, 4, 8, 16, and 24-hour intervals.

2.9 Statistical analysis

Data are presented as mean ± standard error (SE, n = 3) and were calculated using Microsoft Excel 2019 software. Statistical analysis was performed using SPSS for analysis of variance (ANOVA). Visualization of results was conducted

using Origin Pro 2021 and R Studio for clear and concise presentation in academic publications.

3 Results and discussion

3.1 Association between flower bud/floret size and developmental stage of microspores

The size of floral buds determines the developmental stage of microspores, influencing the success rate of anther tissue culture[43,44]. Cytological observation of *L. japonica* floral buds revealed distinct developmental stages of microspores: tetrad, early-uninucleate, late-uninucleate peripheral, and binucleate stages, corresponding to buds of different sizes (Fig. 1A-J). Floral buds reaching 0.5–0.7 cm in length, displaying greenish coloration with short corollas, predominantly contain microspores at the tetrad stage (Fig. 1C, G). With buds elongating to 1.0-1.4 cm, displaying greenish coloration with elongated corollas, most microspores progress to the early-uninucleate stage (Fig. 1D, H). Subsequently, at lengths of 1.8–2.6 cm (Fig. 1E, I), accompanied by notable elongation of corollas and lightening of green coloration, the majority of microspores reach the late-uninucleate stage. Finally, when buds reach 2.8–3.8 cm in length, displaying a yellowish-green hue and corolla length triple that of the calyx, microspores are predominantly in the binucleate stage (Fig. 1F, J). Studies by Kumar and Alan have indicated that anther cultures containing microspores at the late-uninucleate peripheral stage exhibit the highest yield of embryos, shoots, and haploids when cultured on MS basal medium[45,46]. In this experiment, the induction rate of callus tissue was highest at 78% when microspores in the anthers were at the late-uninucleate peripheral stage, 6.5 times higher than that at the binucleate stage. Additionally, the browning rate was lowest at 15% during this stage, showing a significant difference compared to the other three stages (Table 1). Previous studies have reported lower induction rates when anthers at the binucleate stage are used for cell culture, attributed to the deposition of starch and other storage materials in the late stage of microspore development, often leading to loss of embryogenic potential[47,48]. These findings are consistent with our study results.

Table 1
Induction of anther callus from different developmental stages of microspores in *L. japonica*.

Stage	Induction rate (%)	Browning rate (%)	Contamination rate (%)
Tetrad stage	13 ± 0.40^{c}	72 ± 0.29^{a}	23 ± 0.84^{a}
Early-uninucleate stage	38 ± 0.70^{b}	52 ± 0.89^{b}	10 ± 0.37^{ab}
Late-uninucleate stage	78 ± 0.29^{a}	15 ± 0.27^{c}	7 ± 0.30^{b}
Binucleate stage	12 ± 0.25^{c}	85 ± 0.31^{a}	3 ± 0.15b

Values within each column sharing different letters are significantly different according to Duncan's multiple range tests ($p < 0.05$)

3.2 Callus induction

Plant growth regulators (PGRs) concentrations were optimized using an L_9 (3^4) orthogonal design to induce callus formation and morphogenic characteristics in *L. japonica*. Predominantly used PGRs included auxins (NAA, 2,4-D, IBA) and cytokinins (6-BA, KT), as extensively documented[49,50]. Various combinations of PGRs concentrations facilitated callus induction. However, their effects on induction rate and morphogenic characteristics differed significantly, emphasizing the importance of appropriate PGRs combinations in promoting the initiation and growth of anther-derived callus in H. sabdariffa, consistent with recent findings[51]. Therefore, optimizing the ratio of PGRs is crucial for

establishing a regeneration system in *L. japonica*. This study's results indicate that under different PGRs combinations, the callus induction rate ranged from 9–81%, with distinct variations in callus color observed (Table 2). Variance analysis from the orthogonal experiment (Table 3) revealed that NAA was the primary hormone influencing callus formation and growth, followed by 6-BA, 2,4-D, and KT, all reaching significant levels ($p < 0.05$). However, the theoretical value of $A_2B_3C_3D_1$ differs from the combination $A_2B_3C_1D_2$ in Table 2. Consequently, a comparative analysis between $A_2B_3C_1D_2$ and $A_2B_3C_3D_1$ was conducted, revealing that the induction rate of $A_2B_3C_3D_1$ was 89% and yellowish friable callus characteristics, establishing it as the optimal PGRs combination. Furthermore, the results of this study suggest that higher concentrations of NAA promote the formation of callus tissues, consistent with the findings of Wu et al[52]. and Rout et al[53]. Additionally, studies have shown that yellow and loose callus tissues are rich in secondary metabolites, making them valuable and sustainable raw materials in commercial markets[54,55].

Table 2
Effect of NAA, 2,4-D, KT, 6-BA variables on anther-induced callus.

Test No.	A(6-BA) $mg{\cdot}L^{-1}$	B(NAA) $mg{\cdot}L^{-1}$	C(2,4-D) $mg{\cdot}L^{-1}$	D(KT) $mg{\cdot}L^{-1}$	Induction rate (%)	Callus characteristics
	1(0.5)	1(0.5)	1(0.5)	1(0.2)	17 ± 0.30^{e}	Yellowish-white, watery
	1(0.5)	2(1.0)	3(1.5)	2(0.5)	49 ± 0.38^{c}	Light brown, loose
	1(0.5)	3(1.5)	2(1.0)	3(0.8)	69 ± 0.38^{b}	green, slightly brown, less friable
	2(1.0)	1(0.5)	3(1.5)	3(0.8)	31 ± 0.31^{d}	Yellow-white, loose
	2(1.0)	2(1.0)	2(1.0)	1(0.2)	64 ± 0.34^{b}	White-green, slightly brown,compact
	2(1.0)	3(1.5)	1(0.5)	2(0.5)	81 ± 0.23^{a}	Yellow, friable
	3(1.5)	1(0.5)	2(1.0)	2(0.5)	9 ± 0.23^{e}	White-brown, slightly watery
	3(1.5)	2(1.0)	1(0.5)	3(0.8)	18 ± 0.25^{e}	Yellowish-white, slightly watery
	3(1.5)	3(1.5)	3(1.5)	1(0.2)	70 ± 0.33^{b}	White-green, compact

K ij shows the average response of each factor at different levels where i represent a factor and j a level. Rj = maxzKij -minKij for each factor. NAA, naphthalene acetic acid; 2,4-D, 2,4-dichlorophenoxy acetic acid; 6-BA, 6–benzyladenine; KT, kinetin.

a Variable was coded at 1 level (low) by orthogonal design.

b Variable was coded at 2 level (center) by orthogonal design.

c Variable was coded at 3 level (high) by orthogonal design.

Table 3
ANOVA analysis and Range analysis on anther-induced callus obtained from the $L_9(3^4)$ orthogonal experiment.

Analytical method	A(6-BA) $mg{\cdot}L^{-1}$	B(NAA) $mg{\cdot}L^{-1}$	C(2,4-D) $mg{\cdot}L^{-1}$	D(KT) $mg{\cdot}L^{-1}$
ANOVA analysis				
Df	2	2	2	2
MS	0.52	2.22	0.105	0.093
P value	0.0001**	0.0001**	0.0001**	0.0001**
Range analysis				
k1	0.45	0.19	0.39	0.50
k2	0.59	0.44	0.47	0.46
k3	0.32	0.73	0.50	0.39
Rj	0.26	0.54	0.11	0.09
Best level	A_2	B_3	C_3	D_1

3.3 Callus Proliferation

After transferring 0.5 g of yellow and loose callus tissue onto fresh culture medium identical to that used for induction, it was observed that the hormone ratios optimized for induction were not suitable for subsequent subculture. Consequently, an optimization of plant growth regulator (PGRs) combinations for subculture was conducted based on an L_9 (3^4) orthogonal experiment. In Table S1 combination $A_2B_3C_1D_2$ exhibited the highest fresh weight. Additionally, according to the Rj value analysis (Table S2), the hierarchical influence of PGRs on callus induction was ranked as B > A > C > D, consistent with the ANOVA results. The $A_2B_3C_1D_2$ combination aligned closely with theoretical values, confirming its efficacy. Therefore, the optimal PGRs combination for subculture was determined to be 2.0 $mg{\cdot}L^{-1}$ of 6-benzylaminopurine (6-BA), 0.5 $mg{\cdot}L^{-1}$ of naphthaleneacetic acid (NAA), and 0.2 $mg{\cdot}L^{-1}$ of kinetin (KT). Compared to induction, subculture necessitates higher concentrations of cytokinins, which promote cell division and bud formation[56].

3.4 Histological observations

The selection of embryogenic callus is crucial for the success of subculture in plant tissue culture[57]. Callus formed from explants displays irregular shapes, colors, and varying sizes and structures. Inducing callus from *L. japonica* anthers yields different types of callus. Type I callus is yellow with a moist and dense surface (Fig. 2A). Type II callus is light yellow with high water content and a loose structure (Fig. 2B). Type III callus is brown with a dry and dense surface (Fig. 2C). Scanning electron microscopy (SEM) shows that the callus surface features small pores, a dense continuous layer, and granular structures (Fig. 2D-F). Surface cells of the three callus types transition from tightly packed spherical to indented, and finally to broken and loose cells. These structures facilitate clear distinction among embryogenic, non-embryogenic, and browning callus. The current research findings are supported by Binte Mostafiz et al[58]. Similarly, Corral-Martínez et al[59]., reported that during embryogenesis, most angiosperms exhibit embryogenic callus with prominent granular and fibrous surface structures. Paraffin section observations reveal that Type I embryogenic callus exhibits uniform cell size, dense cytoplasm, active cell division, visible nuclei, and numerous starch grains (Fig. 2G-H,). Additionally, embryogenic cells were observed developing from globular to cotyledonary embryos (Fig. 2J-L). Starch grains stain green with safranin-fast green stain, while nuclei stain red. Under dark-field optical microscopy, starch grains

exhibit spontaneous green fluorescence (Fig. 2H). In contrast, non-embryogenic callus (Type II and Type III) exhibits uneven cell sizes, chaotic arrangement, fewer nuclei, and notably lacks starch grains (Fig. 2I). Similar histological observations are observed in many plants between embryogenic and non-embryogenic tissues. For instance, in Camellia, embryogenic callus has dense cytoplasm and prominent nuclei, whereas non-embryogenic callus has less dense cytoplasm and fewer nuclei[60]. Similar results have been observed in *Handeliodendron bodinieri L.*[61]. The presence of starch grains in embryogenic callus, but not in non-embryogenic callus, aligns with observations made by Kong et al[62]. Thus, the presence or absence of starch grains provides a convenient tool to identify embryogenic and non-embryogenic tissues. In establishing the regeneration system of *Angelica*, somatic embryos in embryogenic callus were observed to develop from globular to cotyledonary stages[63]. Similar observations were made in *Juglans regia L.* and *Pulsatilla tongkangensis*[64,65].

3.5 The Effect of Different Light Qualities on the Growth and Development of L. japonica Callus.

This study observed surface cell color changes under various light qualities (Fig. 3). After 15 days of cultivation, callus expose to red and blue light turned green. Blue light treatment not only changed the surface color to green but also caused the green color to spread internally. In contrast, red light caused a slower color change, with greening only on the surface, while white light caused no color change. By day 25, callus proliferation continued. The green color deepened under red light but lightened under blue light. After 35 days, callus proliferation under red and blue light slowed. Signs of senescence appeared, and the surface color faded and lost its luster. Additionally, As the cultivation period extended, more brown tissue and white hard cells formed on the callus surface. Senescence was most pronounced under blue light, with a significant increase in brown cells on the callus surface. Lai et al[24]., reported similar findings, noting that callus senescence was most severe under blue light and least under white light.

3.6 The effect of light quality on the content of total phenols, total flavonoids, and soluble sugars.

Phenolic compounds, commonly found in plants, have attracted significant attention because of their antioxidant properties[66,67]. Flavonoids are a major category of phenolic compounds. Soluble sugars, as primary metabolites, play crucial roles in growth regulation, carbon partitioning, photosynthesis, carbohydrate and lipid metabolism, protein synthesis, and gene expression[68,69]. This study investigated how light quality affects the accumulation of phenolics, flavonoids, and soluble sugars in *L. japonica* callus under varying light conditions (Fig. 4). The total phenolic content in *L. japonica* callus varied significantly among different light qualities. Compared to white light, both blue and red light significantly increased the total phenolic content at early (5 days), mid (15 days), and late-mid (25 days) stages of callus culture ($p < 0.05$). Under blue light, the total phenolic content ranged from 16.71 to 32.40 mg/g DW, whereas under red light, it ranged from 15.775 to 28.819 mg/g DW. Blue light resulted in significantly higher phenolic content compared to red light. The highest phenolic content (32.398 mg/g DW) was observed in callus treated with blue light for 15 days. At the late stage of culture (35 days), the phenolic content under white light was 25.408 mg/g DW, 0.069 times higher than that under blue light and 0.23 times higher than that under red light. The total flavonoid content in callus grown under different light qualities varied substantially. Under white light, the total flavonoid content increased with culture duration, reaching a maximum of 6.42 mg/g DW at 35 days. This was not significantly different from the blue light treatment but was 2.01 times higher than red light treatment ($p < 0.05$). Under blue and red light, the total flavonoid content first increased and then decreased, peaking at 7.653 mg/g DW and 5.754 mg/g DW at 15 days, respectively. The flavonoid content under blue light was 0.33 times higher than that under red light. Different light qualities also significantly affected soluble sugar content. Compared to white light, blue light significantly promoted the accumulation of soluble sugars in the early and mid-stage ($p < 0.05$). The maximum soluble sugar content under blue light was 17.779 mg/g DW at the mid stage, 0.20 times and 0.51 times higher than under white and red light, respectively. However, in the late-mid and late stages, blue light inhibited soluble sugar accumulation. Red light only promoted soluble sugar accumulation at the early

stage, with a content of 14.868 mg/g DW. Under white light, soluble sugar content increased with culture duration, reaching a maximum of 16.443 mg/g DW at the late stage. These results demonstrate that blue light significantly enhances the accumulation of total phenolics, flavonoids, and soluble sugars in *L. japonica* callus cultured for 15 days There is substantial evidence that blue light induces the accumulation of total phenolics, flavonoids, and soluble sugars[22,70,71,72]. Studies have shown that blue light promotes the expression of PAL, a key enzyme in the phenylpropanoid biosynthesis pathway[34]. Therefore, blue light plays a significant role in the biosynthetic pathway of metabolites, leading to the accumulation of phenolic compounds[73]. Previous reports have also indicated that blue light stimulates the total phenolic content (TPC) and total flavonoid content (TFC) in callus cultures of *Rhodiola imbricata* and *Stevia rebaudiana*[70,22]. LED blue light improved soluble sugar accumulation in non-heading Chinese cabbage[71]. Blue light induction also stimulated soluble sugar accumulation in *Hyoscyamus reticulatus*[72].

3.7 Effect of light quality on antioxidant capacity

DPPH and FRAP assays are widely used to evaluate the antioxidant potential of extracts or other biological sources due to their simplicity, robustness, and reliability[74,75]. In this study, we assessed the antioxidant capacity of callus cultures grown under different light qualities using the DPPH radical scavenging activity (Fig. 5A). Compared to white light, both blue and red light significantly promoted DPPH radical scavenging activity in the early (5 days), mid (15 days), and late-mid stages (25 days), with blue light showing higher DPPH values than red light ($p < 0.05$). At the mid-stage, the DPPH value under blue light reached 70.25%, which was significantly higher than under white and red light by 63.4% and 2.15%, respectively ($p < 0.05$). At the late stage (35 days), red light significantly inhibited DPPH radical scavenging activity, while there was no significant difference between blue and white light, with DPPH values of 60.34% and 60.60%, respectively. Ferric Reducing Antioxidant Power (FRAP) assay also exhibited significant variations (Fig. 5B). Compared to white light, blue light significantly enhanced the antioxidant capacity of callus cultures during the first three stages (5, 15, 25 days). The highest antioxidant capacity was observed at the mid-stage, being 0.96 times that of white light ($p < 0.05$) and 0.23 times that of red light ($p > 0.05$). Red light significantly increased the μantioxidant capacity of callus cultures in the mid and late stages, with FRAP values increasing by 59.4% and 27.1%, respectively, compared to white light ($p < 0.05$). At the late stage the FRAP value of callus cultures under white light was 437.882 μmol Fe (II)/L DW, which was 1.92 times higher than under red light ($p < 0.05$) and not significantly different from blue light ($p > 0.05$). Our results are consistent with Biswal et al[76]., who reported a similar enhancement of antioxidant capacity in callus cultures of *Operculina turpethum (L.)* grown under blue light. Similarly, Azad et al[77]., demonstrated higher DPPH and FRAP activities in soybeans treated with blue light. These findings underscore the significant role of blue light in enhancing the antioxidant capacity of callus cultures, as evidenced by increased DPPH and FRAP activities.

3.8 Chromatographic fingerprint analysis

The chromatographic fingerprint can comprehensively qualify and quantify various chemical constituents of Traditional Chinese Medicine (TCM). High-Performance Liquid Chromatography (HPLC) remains the primary method for TCM quality control due to its good reproducibility, wide application, and high efficiency[78]. At a detection wavelength of 245 nm, the chromatographic peaks exhibit high resolution, symmetrical shape, and a stable baseline, which are conducive to establishing the fingerprint profile. Sample S1 was selected for methodological validation, and the relative standard deviations (RSD) for precision, repeatability, and stability were all below 3.8%, indicating that the established method is suitable for constructing the HPLC fingerprint of *L. japonica*. The chromatograms were imported into the “Similarity Evaluation System for Chromatographic Fingerprint of Traditional Chinese Medicine (2012 edition)” software, setting the reference spectrum. Through automatic matching and multipoint calibration, the common peaks were matched, and the standard fingerprint was generated[79]. The standard fingerprint profile of *L. japonica* callus tissue is shown in Fig S1A. Based on the chromatographic peak matching information, 11 common peaks were identified. Similarity analysis revealed that the similarity values between the samples treated with different light qualities and the standard fingerprint

profile ranged from 0.872 to 0.991, indicating some degree of variation in the chemical composition of the callus tissue under different light conditions. The similarity values are presented in Table 4.

Table 4
The similarity values of *L. japonica* in different light qualities.

NO.	S1	S2	S3	S4	S5	S6	S7	S8	S9	S10	S11	S12	R
S1	1												
S2	0.976	1											
S3	0.984	0.982	1										
S4	0.983	0.987	0.995	1									
S5	0.935	0.907	0.896	0.919	1								
S6	0.972	0.929	0.962	0.955	0.939	1							
S7	0.843	0.805	0.808	0.833	0.928	0.856	1						
S8	0.956	0.985	0.975	0.977	0.856	0.897	0.755	1					
S9	0.956	0.948	0.93	0.946	0.922	0.896	0.776	0.936	1				
S10	0.934	0.969	0.955	0.953	0.803	0.859	0.722	0.992	0.902	1			
S11	0.939	0.972	0.958	0.959	0.822	0.868	0.723	0.996	0.92	0.997	1		
S12	0.843	0.77	0.822	0.805	0.861	0.913	0.847	0.704	0.721	0.658	0.653	1	
R	0.991	0.975	0.983	0.987	0.959	0.979	0.887	0.95	0.943	0.921	0.927	0.872	1

3.9 Principal component analysis

Principal Component Analysis (PCA) was performed using SPSS 25.0 statistical software. The peak areas of the 11 common peaks in the HPLC fingerprint were input as 11 variables in the dataset rows, while the sample numbers were input in the dataset columns. The PCA results indicated that the cumulative variance contribution rate of the five principal components reached 90.906% (Table 5). This suggests that the extracted five principal components can effectively represent the original 11 variables. The eigenvalues and contribution rates of the five principal components (PC1-PC5) are shown in Table 5. PCA uses orthogonal transformation to convert a set of possibly correlated variables into a set of linearly uncorrelated variables[80]. The first principal component is defined to have the maximum variance possible, with each subsequent component having the maximum variance possible while being orthogonal to the previous components[81]. PC1, PC2, PC3, PC4, and PC5 contribute 34.009%, 22.028%, 15.205%, 11.856%, and 7.809% to the total variance of the input variables, respectively. These five principal components explain 90.906% of the total information. The initial factor loading matrix was further calculated to determine the contribution and direction of each variable to the principal components. As shown in Table S3 peak 3 contributes significantly to PC1, peak 5 to PC2, peak 8 to PC3, peak 8 to PC4, and peak 10 to PC5. Mantel test analysis of the common peaks revealed significant correlations: peak 3 with peaks 6 and 11, and peak 8 with peaks 11, 10, and 2 (Fig. 6). Standard verification identified peaks 3 and 8 as chlorogenic acid and 3,5-dicaffeoylquinic acid A, respectively (Fig. S1B). Therefore, peaks 3 and 8 were used for the analysis of chemical composition content and representative HPLC chromatogram was shown in Fig. 7.

Table 5
Characteristic values and contribution rates of principal components.

Principal component	Characteristic value	Contribution %	Cumulative contribution %
PC1	3.741	34.009	34.009
PC2	2.423	22.028	56.037
PC3	1.673	15.205	71.241
PC4	1.304	11.856	83.097
PC5	0.859	7.809	90.906

3.10 Effects of Light Quality on Chlorogenic acid and 3,5-Dicaffeoylquinic acid

The primary components of *L. japonica* are organic acids. In the 2020 edition of the Chinese Pharmacopoeia[82], chlorogenic acid is used as an index component. The total amount of phenolic acids, including chlorogenic acid ($C_{16}H_{18}O_9$), 3,5-di-O-caffeoylquinic acid ($C_{25}H_{24}O_{12}$), and 4,5-di-O-caffeoylquinic acid ($C_{25}H_{24}O_{12}$), serves as a quality control indicator for *L. japonica*. The content of chlorogenic acid and 3,5-dicaffeoylquinic acid in *L. japonica* callus is affected by the duration of light induction (Fig. 8). As shown in Fig. 8A, red and blue light significantly enhance the synthesis of phenolic compounds in *L. japonica* callus compared to white light. Under blue light, the chlorogenic acid content in callus peaked at 15 days, measuring 12.32 mg/g, which is 4.9 times higher than under white light and 1.6 times higher than under red light. At 25 days, the chlorogenic acid content under red light peaked at 9.74 mg/g, showing no significant difference from blue light ($p > 0.05$) but a highly significant difference from white light ($p < 0.01$), being twice that under white light. Under white light, the chlorogenic acid content increased over the induction period. At 35 days, blue light inhibited chlorogenic acid content, while white light resulted in a content of 6.54 mg/g, 12.95% higher than blue light. The accumulation of 3,5-dicaffeoylquinic acid A in *L. japonica* callus varied significantly under different light qualities at different stages. As shown in Fig. 8B, red and blue light initially increased and then decreased the accumulation of 3,5-dicaffeoylquinic acid A at various stages. At the early and mid-cultivation stage, blue and red light significantly promoted the accumulation of 3,5-dicaffeoylquinic acid A. At the early stage, blue and red light increased the accumulation of 3,5-dicaffeoylquinic acid by 1.98 times and 0.21 times, respectively, compared to white light. At the mid-stage, the accumulation of 3,5-dicaffeoylquinic acid A under blue light reached 7.65 mg/g, which is 2.48 times and 1.24 times higher than under white and red light, respectively. Under white light, the accumulation of 3,5-dicaffeoylquinic acid A increased over time. At 35 days, the content under white light was 6.81 mg/g, which is 5 times and 2 times higher than under blue and red light, respectively. In summary, blue light is the most effective inducer for the accumulation of chlorogenic acid and 3,5-dicaffeoylquinic acid A in *L. japonica* callus, with the optimal cultivation time being 15 days. Our results are consistent with Senekovič et al[83]. who found that blue light induced a higher accumulation of chlorogenic acid compounds in *Berulaerecta* in tissue culture. Studies have shown that blue light can alter the expression patterns of genes related to secondary metabolism[84]. In strawberries, blue light upregulated the main gene FvHCT in the chlorogenic acid synthesis pathway, leading to increased chlorogenic acid content[85]. Blue light induced high expression of phenylalanine ammonia-lyase (PAL) and its product activity, as well as high expression of cinnamate 4-hydroxylase (C4H) and coumarate 3-hydroxylase (C3H) in young lettuce plants, leading to a significant accumulation of chlorogenic acid in the phenylpropanoid pathway[86].

Declarations

Funding

“Star of Innovation” project for graduate students in Gansu Province in 2023 (NO.2023CXZX-648); *Lonicera japonica* Flos seedling breeding and integrated application of cost-saving and efficiency technology (2021YFD11005042); Gansu Youth Science and Technology Fund (23JRRA1444); Youth Doctoral Support Project for Universities in Gansu Province in 2023 (2023QB-125); Research Program Sponsored by State Key Laboratory of Aridland Crop Science, Gansu Agricultural University (GSCS-2023-13); Lanzhou Youth Science and Technology Talent Innovation Project of Lanzhou Science and Technology Bureau (2023-ON-162); Gansu Agricultural University Public Recruitment Doctoral Research Launch Fund (GAU-KYQD-2022-07); Agricultural Science and Technology Innovation Capability Construction Project of the Ministry of Agriculture and Rural Affairs (2109-00000020-01-199092).

Author Contribution

J.C:Investigation, Methodology, Formal analysis, Conceptualization, Sample preparation, Data curation, Data analysis, Writing-original draft.F.G:Methodology, Sample preparation.C.Z and Y.C:Investigation.Z.L , H.W and W.L:Formal analysis.Y.C and P.D:Writing-review & editing.

ACKNOWLEDGMENTS

The authors are grateful to the Department of Chinese Herbal Medicine, College of Agriculture, and the State Key Laboratory of Aridland Crop Science in Gansu Agricultural University for providing the experimental platform.

Supporting Information

Orthogonal test results of PGRs affect callus subculture (Table S1); ANOVA analysis and Range analysis on callus subculture obtained from the $L_9(3^4)$ orthogonal experiment (Table S2); Factor load matrix (Table S3). The standard fingerprints of *L. japonica* in different light quality (Fig S1).

Notes

The authors declare no competing financial interest.

References

1. Zhu W, et al. Variations of Metabolites and Proteome in *Lonicera Japonica Thunb*. Buds and Flowers under UV Radiation. Biochim. Biophys Acta BBA - Proteins Proteom. 2017;1865(4):404–13. https://doi.org/10.1016/j.bbapap.2017.01.004.
2. Li Y, Li W, Fu C, Song Y, Fu Q. *Lonicerae Japonicae* Flos and *Lonicerae* Flos: A Systematic Review of Ethnopharmacology, Phytochemistry and Pharmacology. Phytochem Rev. 2020;19(1):1–61. https://doi.org/10.1007/s11101-019-09655-7.
3. Kang OH, et al. Inhibition of Trypsin-Induced Mast Cell Activation by Water Fraction of *Lonicera Japonica*. Arch Pharm Res. 2004;27(11):1141–6. https://doi.org/10.1007/BF02975120.
4. Park HS, et al. Polyphenolic Extract Isolated from Korean *Lonicera Japonica* Thunb. Induce G2/M Cell Cycle Arrest and Apoptosis in HepG2 Cells: Involvements of PI3K/Akt and MAPKs. Food Chem Toxicol. 2012;50(7):2407–16. https://doi.org/10.1016/j.fct.2012.04.034.
5. RYU KH, et al. Anti-Inflammatory and Analgesic Activities of SKLJI, a Highly Purified and Injectable Herbal Extract of *Lonicera Japonica*. Biosci Biotechnol Biochem. 2010;74(10):2022–8. https://doi.org/10.1271/bbb.100279.

6. Zhang F, et al. A Simple, Rapid, and Practical Method for Distinguishing *Lonicerae Japonicae* Flos from *Lonicerae* Flos. Molecules. 2019;24(19). https://doi.org/10.3390/molecules24193455.
7. Zhang M, et al. Exploration of Exogenous Chlorogenic Acid as a Potential Plant Stimulant: Enhancing Physiochemical Properties in *Lonicera Japonica*. Physiol Mol Biol Plants. 2024;30(3):453–66. https://doi.org/10.1007/s12298-024-01435-8.
8. Sun C, et al. Metabonomics Study of the Protective Effects of *Lonicera Japonica* Extract on Acute Liver Injury in Dimethylnitrosamine Treated Rats. J Pharm Biomed Anal. 2010;53(1):98–102. https://doi.org/10.1016/j.jpba.2010.03.015.
9. Wang T, et al. Transcriptional Regulation of *Lonicera Japonica* Thunb. during Flower Development as Revealed by Comprehensive Analysis of Transcription Factors. BMC Plant Biol. 2019;19(1):198. https://doi.org/10.1186/s12870-019-1803-1.
10. Dias MC, Pinto DCGA, Silva AMS. Plant Flavonoids: Chemical Characteristics and Biological Activity. Molecules. 2021;26(17). https://doi.org/10.3390/molecules26175377.
11. Chen L, Cao H, Huang Q, Xiao J, Teng H, Absorption. Metabolism and Bioavailability of Flavonoids: A Review. Crit Rev Food Sci Nutr. 2022;62(28):7730–42. https://doi.org/10.1080/10408398.2021.1917508.
12. Fang Z, Li J, Yang R, Fang L, Zhang YA, Review. The Triterpenoid Saponins and Biological Activities of *Lonicera* Linn. Molecules. 2020;25(17). https://doi.org/10.3390/molecules25173773.
13. Lai KH, et al. *Lonicerae Japonicae* Flos Attenuates Neutrophilic Inflammation by Inhibiting Oxidative Stress. Antioxidants. 2022;11(9). https://doi.org/10.3390/antiox11091781.
14. Hu M, et al. Establishment of Cell Suspension Culture of *Lonicera Japonica* Thunb and Analysis Its Major Secondary Metabolites. Ind Crops Prod. 2019;137:98–104. https://doi.org/10.1016/j.indcrop.2019.05.024.
15. Pan Y, et al. Callus growth kinetics and accumulation of secondary metabolites of *Bletilla striata* Rchb.f. using a callus suspension culture. PLoS ONE. 2020;15(2):e0220084. https://doi.org/10.1371/journal.pone.022008.
16. Buranasudja V, Rani D, Malla A, Kobtrakul K, Vimolmangkang S. Insights into Antioxidant Activities and Anti-Skin-Aging Potential of Callus Extract from *Centella Asiatica* (L). Sci Rep. 2021;11(1):13459. https://doi.org/10.1038/s41598-021-92958-7.
17. Yang L, et al. Response of Plant Secondary Metabolites to Environmental Factors. Molecules. 2018;23:762. https://doi.org/10.3390/molecules2304076.
18. Narayani M, Srivastava S, Elicitation. A Stimulation of Stress in in Vitro Plant Cell/Tissue Cultures for Enhancement of Secondary Metabolite Production. Phytochem Rev. 2017;16(6):1227–52. https://doi.org/10.1007/s11101-017-9534-0.
19. Huang P, et al. Influence of Different Elicitors on BIA Production in *Macleaya Cordata*. Sci Rep. 2021;11(1):619. https://doi.org/10.1038/s41598-020-79802-0.
20. Akula R, Ravishankar GA. Influence of Abiotic Stress Signals on Secondary Metabolites in Plants. Plant Signal Behav. 2011;6(11):1720–31. https://doi.org/10.4161/psb.6.11.17613.
21. Tariq U, Ali M, Abbasi BH. Morphogenic and Biochemical Variations under Different Spectral Lights in Callus Cultures of *Artemisia Absinthium* L. J Photochem Photobiol B. 2014;130:264–71. https://doi.org/10.1016/j.jphotobiol.2013.11.026.
22. Ahmad N, Rab A, Ahmad N. Light-Induced Biochemical Variations in Secondary Metabolite Production and Antioxidant Activity in Callus Cultures of *Stevia Rebaudiana* (Bert). J Photochem Photobiol B. 2016;154:51–6. https://doi.org/10.1016/j.jphotobiol.2015.11.015.
23. Fazal H, et al. Correlation of Different Spectral Lights with Biomass Accumulation and Production of Antioxidant Secondary Metabolites in Callus Cultures of Medicinally Important *Prunella Vulgaris* L. J Photochem Photobiol B.

2016;159:1–7. https://doi.org/10.1016/j.jphotobiol.2016.03.008.

24. Lai CC, et al. Light Quality Modulates Growth, Triggers Differential Accumulation of Phenolic Compounds, and Changes the Total Antioxidant Capacity in the Red Callus of *Vitis Davidii*. J Agric Food Chem. 2022;70(41):13264–78. https://doi.org/10.1021/acs.jafc.2c04620.
25. Hayta S, et al. Induction of *Gentiana Cruciata* Hairy Roots and Their Secondary Metabolites. Biol (Bratisl. 2011;66(4):618–25. https://doi.org/10.2478/s11756-011-0076-4.
26. Singh J et al. Enhanced Secondary Metabolite Production and Pathway Gene Expression by Leaf Explants-Induced Direct Root Morphotypes Are Regulated by Combination of Growth Regulators and Culture Conditions in *Centella Asiatica* (L.) Urban. Plant Growth Regul. 2015, 75 (1), 55–66. https://doi.org/10.1007/s10725-014-9931-y
27. Azeez H, et al. Changes Induced by Gamma Ray Irradiation on Biomass Production and Secondary Metabolites Accumulation in *Hypericum Triquetrifolium* Turra Callus Cultures. Ind Crops Prod. 2017;108:183–9. https://doi.org/10.1016/j.indcrop.2017.06.040.
28. Karakas FP. Efficient Plant Regeneration and Callus Induction from Nodal and Hypocotyl Explants of Goji Berry (*Lycium Barbarum* L.) and Comparison of Phenolic Profiles in Calli Formed under Different Combinations of Plant Growth Regulators. Plant Physiol Biochem. 2020;146:384–91. https://doi.org/10.1016/j.plaphy.2019.11.009.
29. Maharani A, Fanata WID, Laeli FN, Kim K-M, Handoyo T. Callus Induction and Regeneration from Anther Cultures of Indonesian Indica Black Rice Cultivar. J Crop Sci Biotechnol. 2020;23(1):21–8. https://doi.org/10.1007/s12892-019-0322-0.
30. Popielarska-Konieczna M, et al. Ultrastructure and Histochemical Analysis of Extracellular Matrix Surface Network in Kiwifruit Endosperm-Derived Callus Culture. Plant Cell Rep. 2008;27(7):1137–45. https://doi.org/10.1007/s00299-008-0534-9.
31. Liu X, et al. Establishment of Callus Induction System, Histological Evaluation and Taxifolin Production of Larch. Plant Cell Tissue Organ Cult PCTOC. 2021;147(3):467–75. https://doi.org/10.1007/s11240-021-02139-7.
32. Li M, et al. Temperature-Regulated Anatomical and Gene-Expression Changes in *Sinopodophyllum Hexandrum* Seedlings. Ind Crops Prod. 2020;152:112479. https://doi.org/10.1016/j.indcrop.2020.112479.
33. Liu X, Luo M, Li M, Wei J. Depicting Precise Temperature and Duration of Vernalization and Inhibiting Early Bolting and Flowering of *Angelica Sinensis* by Freezing Storage. Front Plant Sci. 2022;13:853444. https://doi.org/10.3389/fpls.2022.853444.
34. Yao W, et al. Effect of Different Culture Conditions on Anthocyanins and Related Genes in Red Pear Callus. Agronomy. 2023;13(8). https://doi.org/10.3390/agronomy13082032.
35. Lay MM, Karsani SA, Mohajer S, Abd Malek SN, Phytochemical Constituents. Nutritional Values, Phenolics, Flavonols, Flavonoids, Antioxidant and Cytotoxicity Studies on *Phaleria Macrocarpa* (Scheff.) Boerl Fruits. BMC Complement. Altern. Med. 2014, 14 (1), 152. https://doi.org/10.1186/1472-6882-14-152
36. Han Z, et al. Association Mapping for Total Polyphenol Content, Total Flavonoid Content and Antioxidant Activity in Barley. BMC Genomics. 2018;19(1):81. https://doi.org/10.1186/s12864-018-4483-6.
37. Villamarin-Raad DA, et al. Changes in Phenolic Profile and Total Phenol and Total Flavonoid Contents of Guadua *Angustifolia Kunth* Plants under Organic and Conventional Fertilization. ACS Omega. 2023;8(44):41223–31. https://doi.org/10.1021/acsomega.3c04579.
38. Chow PS, Landhäusser SM. A Method for Routine Measurements of Total Sugar and Starch Content in Woody Plant Tissues. Tree Physiol. 2004;24(10):1129–36. https://doi.org/10.1093/treephys/24.10.1129.
39. Thaipong K, Boonprakob U, Crosby K, Cisneros-Zevallos L, Byrne DH. Comparison of ABTS, DPPH, FRAP, and ORAC Assays for Estimating Antioxidant Activity from Guava Fruit Extracts. J Food Compos Anal. 2006;19(6):669–75. https://doi.org/10.1016/j.jfca.2006.01.003.

40. Jha DK, Panda L, Ramaiah S, Anbarasu A. Evaluation and Comparison of Radical Scavenging Properties of Solvent Extracts from *Justicia Adhatoda* Leaf Using DPPH Assay. Appl Biochem Biotechnol. 2014;174(7):2413–25. https://doi.org/10.1007/s12010-014-1164-z.
41. Sethi S, et al. Significance of FRAP, DPPH, and CUPRAC Assays for Antioxidant Activity Determination in Apple Fruit Extracts. Eur Food Res Technol. 2020;246(3):591–8. https://doi.org/10.1007/s00217-020-03432-z.
42. Chaves N, Santiago A, Alías JC. Quantification of the Antioxidant Activity of Plant Extracts: Analysis of Sensitivity and Hierarchization Based on the Method Used. Antioxidants. 2020;9(1). https://doi.org/10.3390/antiox9010076.
43. Germanà MA. Anther Culture for Haploid and Doubled Haploid Production. Plant Cell Tissue Organ Cult PCTOC. 2011;104(3):283–300. https://doi.org/10.1007/s11240-010-9852-z.
44. Bhatia R et al. Optimizing Protocol for Efficient Microspore Embryogenesis and Doubled Haploid Development in Different Maturity Groups of Cauliflower (*B. Oleracea* Var. *Botrytis* L.) in India. Euphytica. 2016, 212 (3), 439–454. https://doi.org/10.1007/s10681-016-1775-2
45. Kumar KR, Singh KP, Bhatia R, Raju DVS, Panwar S. Optimising Protocol for Successful Development of *Haploids* in Marigold (Tagetes Spp.) through in Vitro Androgenesis. Plant Cell Tissue Organ Cult PCTOC. 2019;138(1):11–28. https://doi.org/10.1007/s11240-019-01598-3.
46. Alan AR et al. Doubled Haploid Broccoli (*Brassica Olearacea* Var. Italica) Plants from Anther Culture. In Doubled Haploid Technology: Volume 2: Hot Topics, Apiaceae, Brassicaceae, Solanaceae; Segui-Simarro, J. M., Ed.; Springer US: New York, NY, 2021; pp 201–216. https://doi.org/10.1007/978-1-0716-1335-1_12
47. Baliyan N, et al. Correlation of Stages of Microsporogenesis with Bud and Anther Morphology in Pepper Genotypes through DAPI Staining with Different Levels of Mordant in *Cytological Fixative*. Protoplasma. 2024;261(2):367–76. https://doi.org/10.1007/s00709-023-01903-0.
48. Yang K, et al. Carbohydrate Metabolism and Gene Regulation during Anther Development in an Androdioecious Tree, *Tapiscia Sinensis*. Ann Bot. 2017;120(6):967–77. https://doi.org/10.1093/aob/mcx094.
49. Yuliani F, Dewi WS, Yunus A, Siswanto U. The study of artemisinin content in callus *Artemisia annua* L. cultures elicited with endophytic fungi aspergillus sp. Molekul. 2018;13:155. https://doi.org/10.20884/1.jm.2018.13.2.459.
50. Zayova E, et al. Tissue Culture Applications of *Artemisia Annua* L. Callus for Indirect Organogenesis and Production Phytochemical. Plant Tissue Cult Biotechnol. 2020;30(1):97–106. https://doi.org/10.3329/ptcb.v30i1.47795.
51. Iiyama CM, Sartoratto A, Cardoso JC. Tissue-Specific and Novel Secondary Metabolites Identified by SPME/GC-MS in *Artemisia Annua* Calli Cultured under Different Wavelength. Ind Crops Prod. 2024;208:117767. https://doi.org/10.1016/j.indcrop.2023.117767.
52. Jamil SZMR, Rohani ER, Baharum SN, Noor NM. Metabolite Profiles of Callus and Cell Suspension Cultures of *Mangosteen*. 3 Biotech 2018, 8 (8), 322. https://doi.org/10.1007/s13205-018-1336-6
53. Efferth T, Engineering Biotechnology Applications of Plant Callus Cultures. 2019, 5 (1), 50–59. https://doi.org/10.1016/j.eng.2018.11.006
54. Wu S, Zu Y, Wu M. High Yield Production of Salidroside in the Suspension Culture of *Rhodiola Sachalinensis*. J Biotechnol. 2003;106(1):33–43. https://doi.org/10.1016/j.jbiotec.2003.07.009.
55. Rout P, et al. Doubled Haploids Generated through Anther Culture from an Elite Long Duration Rice Hybrid, CRHR32: Method Optimization and Molecular Characterization. Plant Biotechnol. 2016;33(3):177–86. https://doi.org/10.5511/plantbiotechnology.16.0719a.
56. Ren X, Liu Y, Jeong BR. Callus Induction and Browning Suppression in Tree Peony *Paeonia Ostii* 'Fengdan.' Hortic. Environ Biotechnol. 2020;61(3):591–600. https://doi.org/10.1007/s13580-020-00246-6.
57. Dai L, Han S, Zhang Y, Hao D. Genetic Architecture of Embryogenic Callus Induction in Maize from the Perspective of Population Genomics. Plant Cell Tissue Organ Cult PCTOC. 2022;150(2):345–59. https://doi.org/10.1007/s11240-

022-02284-7.

58. Binte Mostafiz S, Wagiran A. Efficient Callus Induction and Regeneration in Selected Indica Rice. Agronomy 2018, 8, 77. https://doi.org/10.3390/agronomy805007
59. Corral-Martínez P, et al. Live Imaging of Embryogenic Structures in *Brassica Napus* Microspore Embryo Cultures Highlights the Developmental Plasticity of Induced Totipotent Cells. Plant Reprod. 2020;33(3):143–58. https://doi.org/10.1007/s00497-020-00391-z.
60. Zhang M, et al. Direct and Indirect Somatic Embryogenesis Induction in *Camellia Oleifera* Abel. Front. Plant Sci. 2021;12:644389. https://doi.org/10.3389/fpls.2021.644389.
61. Yu Y, et al. Study on the Induction of Somatic Embryogenesis and Morphological Structural Changes during the Development of *Handeliodendron Bodinieri* L. Plant Cell Tissue Organ Cult PCTOC. 2024;156(2):62. https://doi.org/10.1007/s11240-023-02668-3.
62. Kong EYY, Biddle J, Kalaipandian S, Adkins SW. Coconut Callus Initiation for Cell Suspension Culture. Plants. 2023;12:968. https://doi.org/10.3390/plants12040968.
63. Huang T, et al. Vitro Bioactive Metabolite Production and Plant Regeneration of Medicinal Plant *Angelica Sinensis*. Ind Crops Prod. 2023;194:116276. https://doi.org/10.1016/j.indcrop.2023.116276.
64. Fang H, et al. Optimization of the Induction, Germination, and Plant Regeneration System for Somatic Embryos in Apomictic Walnut (*Juglans Regia* L). Plant Cell Tissue Organ Cult PCTOC. 2022;150(2):289–97. https://doi.org/10.1007/s11240-022-02266-9.
65. Zhao X, et al. Shoot Organogenesis and Somatic Embryogenesis in Leaf Tissue of *Pulsatilla Tongkangensis* Y.N. Plant Biotechnol Rep. 2022;16(4):389–400. https://doi.org/10.1007/s11816-021-00727-9. Lee & T.C. Lee
66. Mandal SM, Dias RO, Franco OL. Phenolic Compounds in *Antimicrobial Therapy*. J Med Food. 2017;20(10):1031–8. https://doi.org/10.1089/jmf.2017.0017.
67. Foss K, Przybyłowicz KE, Sawicki T. Antioxidant Activity and Profile of Phenolic Compounds in Selected Herbal Plants. Plant Foods Hum Nutr. 2022;77(3):383–9. https://doi.org/10.1007/s11130-022-00989-w.
68. Yu J, et al. MdCIbHLH1 Modulates Sugar Metabolism and Accumulation in Apple Fruits by Coordinating Carbohydrate Synthesis and Allocation. Hortic. Plant J. 2024. https://doi.org/10.1016/j.hpj.2024.01.007.
69. Julius BT, et al. Maize Carbohydrate Partitioning Defective1 Impacts Carbohydrate Distribution, Callose Accumulation, and Phloem Function. J Exp Bot. 2018;69(16):3917–31. https://doi.org/10.1093/jxb/ery203.
70. Kapoor S, et al. Influence of Light Quality on Growth, Secondary Metabolites Production and Antioxidant Activity in Callus Culture of *Rhodiola Imbricata* Edgew. J Photochem Photobiol B. 2018;183:258–65. https://doi.org/10.1016/j.jphotobiol.2018.04.018.
71. Fan X, et al. Effects of Different Light Quality on Growth, Chlorophyll Concentration and Chlorophyll Biosynthesis Precursors of Non-Heading Chinese Cabbage (*Brassica Campestris* L). Acta Physiol Plant. 2013;35(9):2721–6. https://doi.org/10.1007/s11738-013-1304-z.
72. Hassanpour H. Potential Impact of Red-Blue LED Light on Callus Growth, Cell Viability, and Secondary Metabolism of *Hyoscyamus Reticulatus*. Vitro Cell. Dev Biol - Plant. 2022;58(2):256–65. https://doi.org/10.1007/s11627-021-10232-x.
73. Zhang X, Bian Z, Li S, Chen X, Lu C. Comparative Analysis of Phenolic Compound Profiles, Antioxidant Capacities, and Expressions of Phenolic Biosynthesis-Related Genes in Soybean Microgreens Grown under Different Light Spectra. J Agric Food Chem. 2019;67(49):13577–88. https://doi.org/10.1021/acs.jafc.9b05594.
74. Kedare SB, Singh RP. Genesis and Development of DPPH Method of Antioxidant Assay. J Food Sci Technol. 2011;48(4):412–22. https://doi.org/10.1007/s13197-011-0251-1.

75. Nazir M, et al. Light-Mediated Biosynthesis of Phenylpropanoid Metabolites and Antioxidant Potential in Callus Cultures of Purple Basil (*Ocimum Basilicum* L. Var Purpurascens). Plant Cell Tissue Organ Cult PCTOC. 2020;142(1):107–20. https://doi.org/10.1007/s11240-020-01844-z.
76. Biswal B, Jena B, Giri AK, Acharya L. Monochromatic Light Elicited Biomass Accumulation, Antioxidant Activity, and Secondary Metabolite Production in Callus Culture of *Operculina Turpethum*. Plant Cell Tissue Organ Cult PCTOC. 2022;149(1):123–34. https://doi.org/10.1007/s11240-022-02274-9.
77. Azad MO, Kim WW, Park CH, Cho DH. Effect of Artificial LED Light and Far Infrared Irradiation on Phenolic Compound, Isoflavones and Antioxidant Capacity in Soybean (*Glycine Max* L). Sprout Foods. 2018;7(10). https://doi.org/10.3390/foods7100174.
78. Liu J, Liu H, Dai Z, Ma S. Quality Analysis of Long Dan Xie Gan Pill by a Combination of Fingerprint and Multicomponent Quantification with Chemometrics Analysis. J. Anal. Methods Chem. 2018, 2018 (1), 4105092. https://doi.org/10.1155/2018/4105092
79. Wang Z, et al. Study on Environmental Factors Affecting the Quality of *Codonopsis Radix* Based on MaxEnt Model and All-in-One Functional Factor. Sci Rep. 2023;13(1):20726. https://doi.org/10.1038/s41598-023-46546-6.
80. Liang X, Guo Z, Wang L, Li R, Lin W. Nearly Optimal Stochastic Approximation for Online Principal Subspace Estimation. Sci China Math. 2023;66(5):1087–122. https://doi.org/10.1007/s11425-021-1972-5.
81. Luo G, Chen G, Tian L, Qin K, Qian S. Minimum Noise Fraction versus Principal Component Analysis as a Preprocessing Step for Hyperspectral Imagery Denoising. Can J Remote Sens. 2016;42(2):106–16. https://doi.org/10.1080/07038992.2016.1160772.
82. Chinese Pharmacopoeia Commission. Pharmacopoeia of the People's Republic of China (2020 Edition). China Medical Science; 2020.
83. Senekovič J, Ciringer T, Ambrožič-Dolinšek J, Islamčević Razboršek M. The Effect of Combined Elicitation with Light and Temperature on the Chlorogenic Acid Content, Total Phenolic Content and Antioxidant Activity of *Berula Erecta* in Tissue Culture. Plants. 2024;13(11). https://doi.org/10.3390/plants13111463.
84. Nam TG, Kim D-O, Eom SH. Effects of Light Sources on Major Flavonoids and Antioxidant Activity in Common Buckwheat Sprouts. Food Sci Biotechnol. 2018;27(1):169–76. https://doi.org/10.1007/s10068-017-0204-1.
85. Chen X, et al. Metabolomic and Transcriptomic Analyses Reveal That Blue Light Promotes Chlorogenic Acid Synthesis in Strawberry. J Agric Food Chem. 2020;68(44):12485–92. https://doi.org/10.1021/acs.jafc.0c05020.
86. Endo M, et al. Effects of Light Quality, Photoperiod, CO_2 Concentration, and Air Temperature on Chlorogenic Acid and Rutin Accumulation in Young Lettuce Plants. Plant Physiol Biochem. 2022;186:290–8. https://doi.org/10.1016/j.plaphy.2022.07.010.

Figures

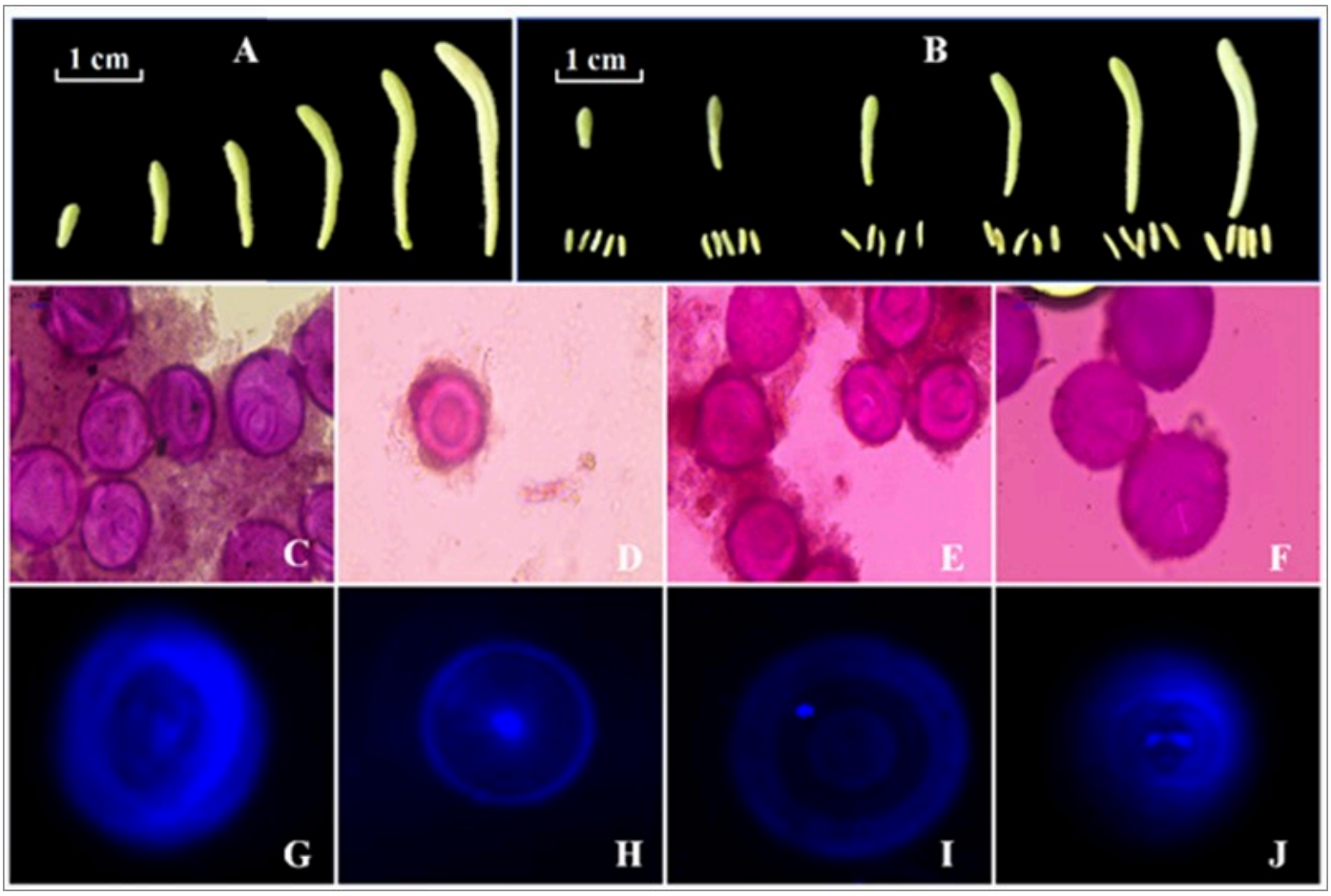


Figure 1

Different sizes of flower buds correspond to the developmental stages of microspores. A-B represents flower buds of different sizes; C-J depict cytological features of the developmental stages of microspores in *L. japonica*. C-F are stained with Carnoy's solution; G-J are stained with DAPI. C, G: Tetrad stage; D, H: Early-uninucleate; E, I: Late-uninucleate; F, J: Binucleate stage.

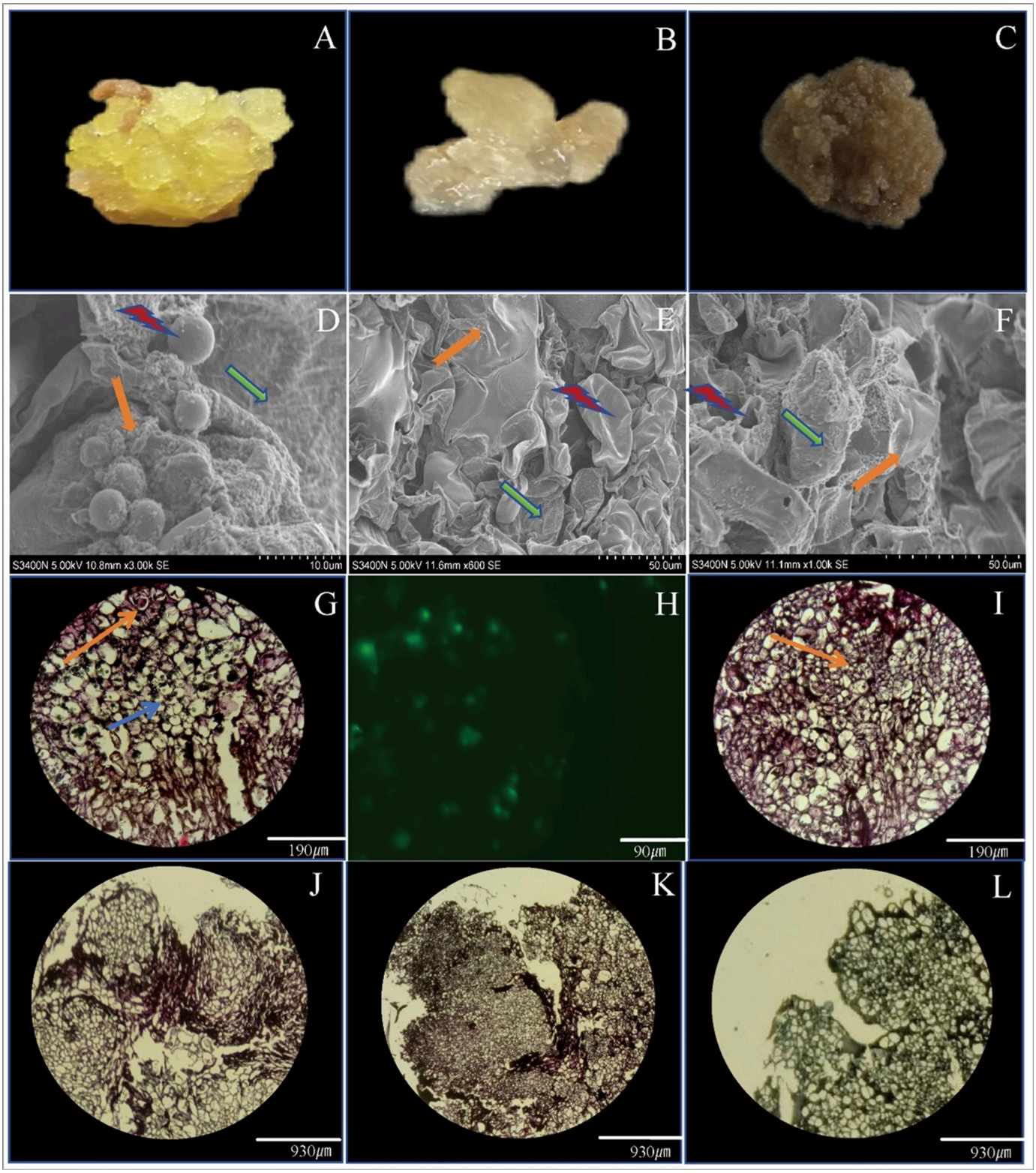


Figure 2

Electron microscopy observation of different morpho-variant callus. A) yellow embryogenic callus, B) light yellow non-embryogenic callus, C) brown necrotic callus. D) Embryogenic callus surface, E) non-embryogenic callus surface, F) necrotic callus surface. The surfaces of these callus tissues exhibit spherical protrusions, depressions leading to ruptures (represented by red lightning), granular structures (represented by orange thick arrows), and membranous layers (represented by green arrows). Safranin-O and fast green staining highlighted nuclei in red and starch grains in green for both embryogenic and non-embryogenic callus tissues (G, I). In embryogenic callus tissues, starch grains emitted green

fluorescence under dark-field microscopy (H). Embryos displaying spherical, heart-shaped, and cotyledonary shapes were observed in embryogenic callus tissues (J-K).

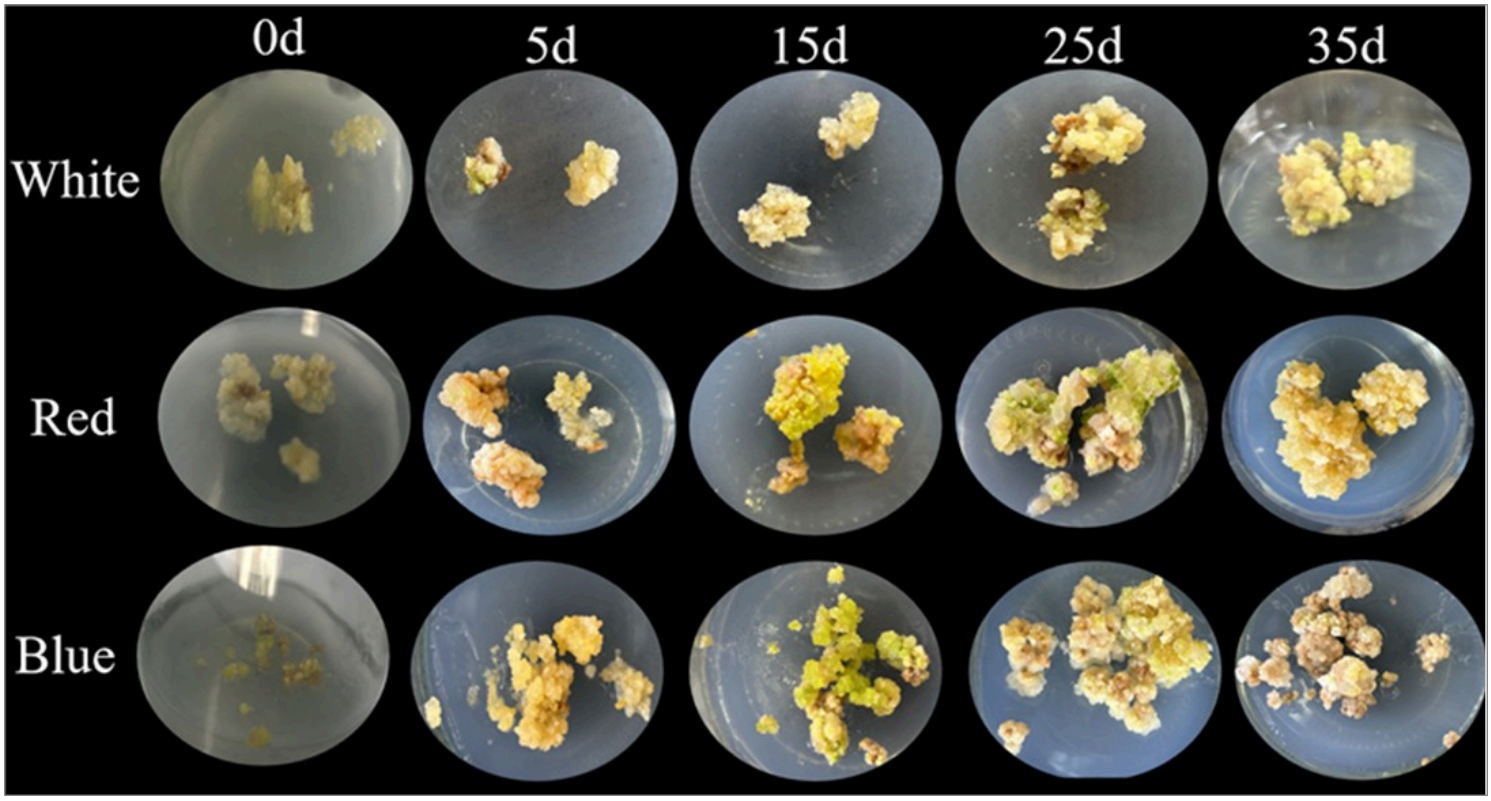


Figure 3

Effects of different light qualities on proliferation of *L. japonica* callus tissues.

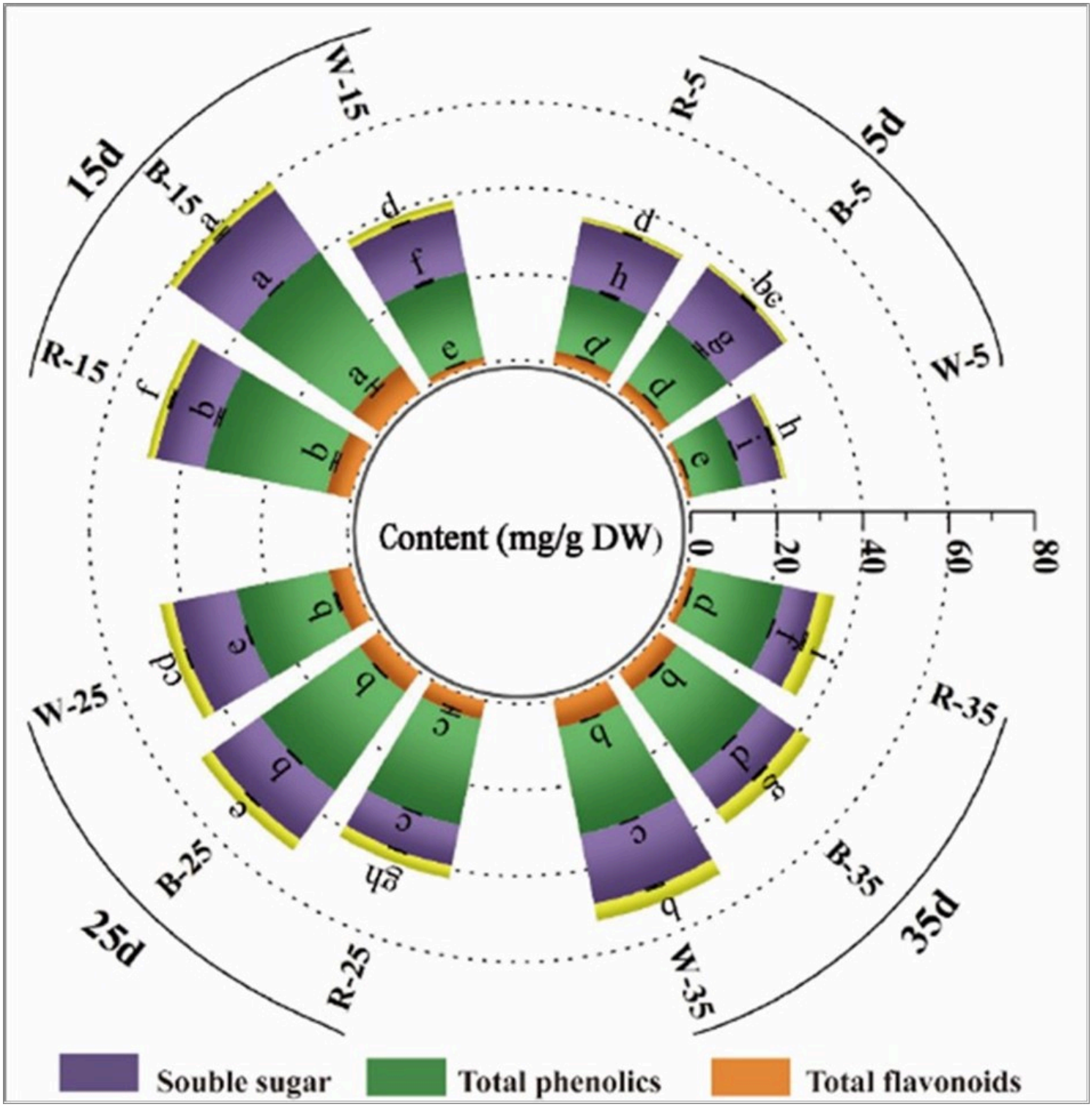


Figure 4

The effects of different light qualities on the total flavonoids, total phenols, and soluble sugar content of *L. japonica* callus tissues were evaluated over a harvest period of 5, 15, 25, and 35 days. Different lowercase letters above the bar chart indicate significant differences in Duncan's new multiple range test at the same culture stage ($p < 0.05$).

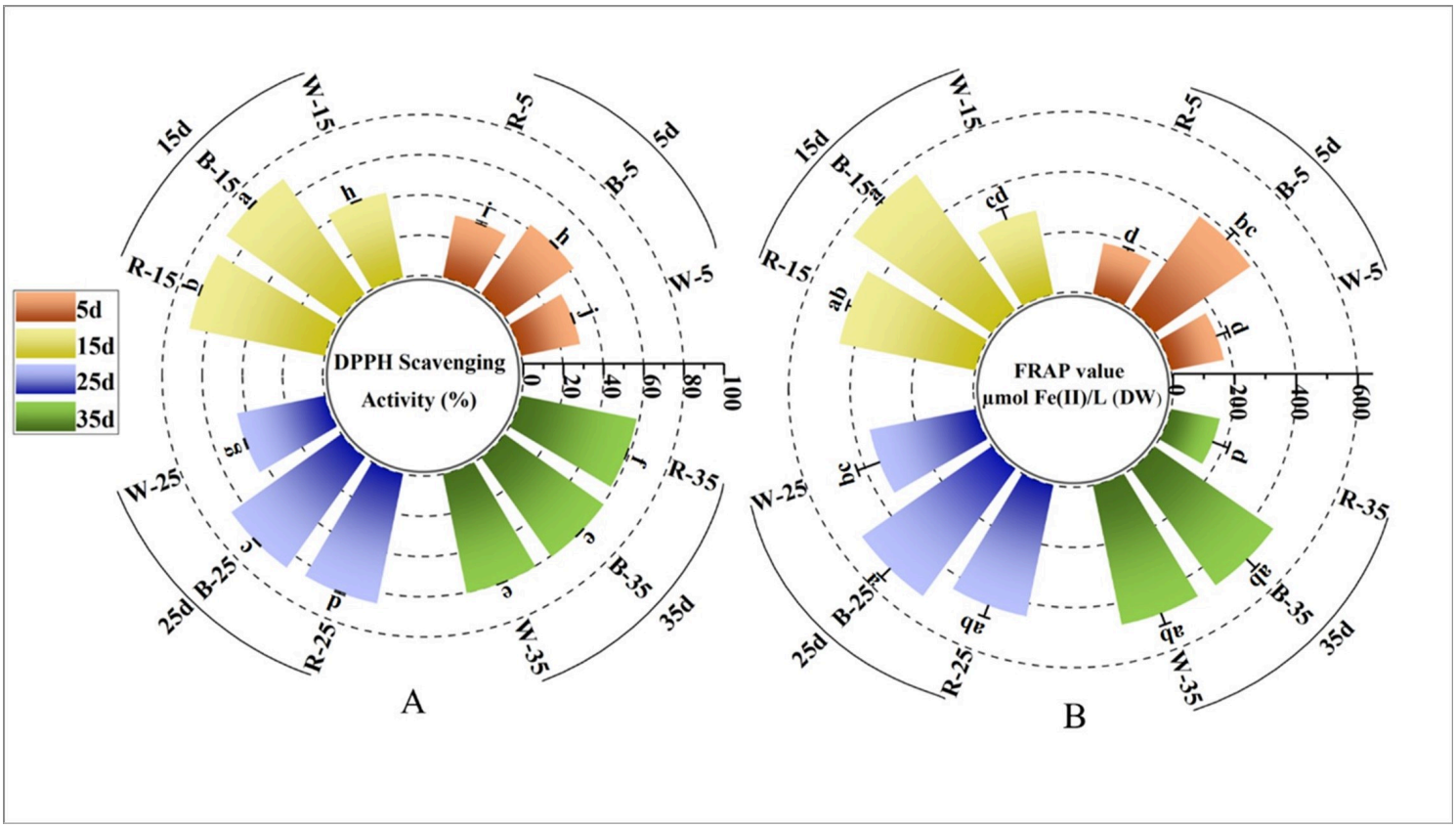


Figure 5

Effects of different light qualities on the DPPH and FRAP content in *L. japonica* callus. Calli were harvested at 5, 15, 25, and 35 days. Different lowercase letters above the bar chart indicate significant differences in Duncan's new multiple range test at the same culture stage ($p < 0.05$).

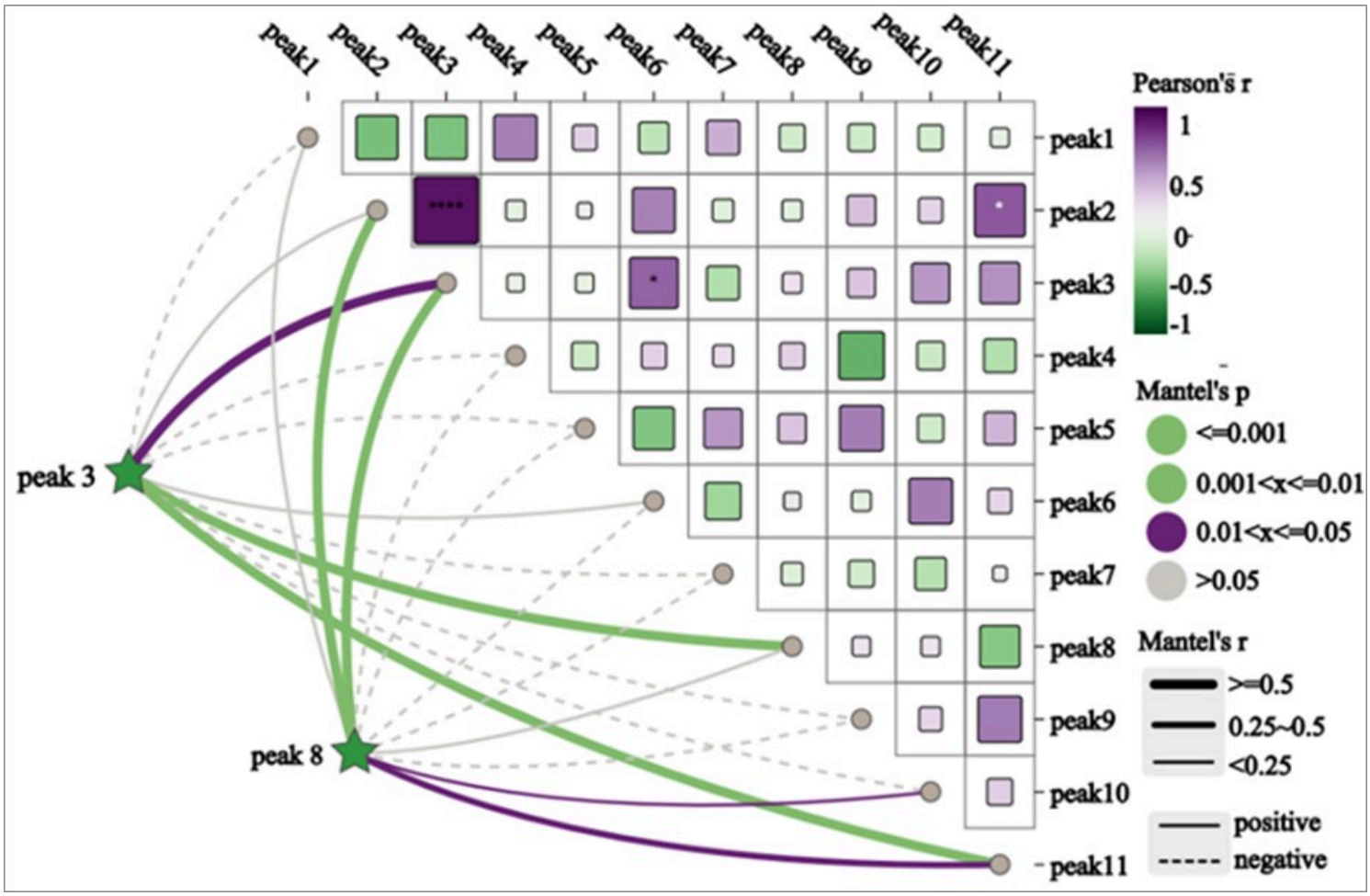


Figure 6

Correlation between common peak-to-peak areas

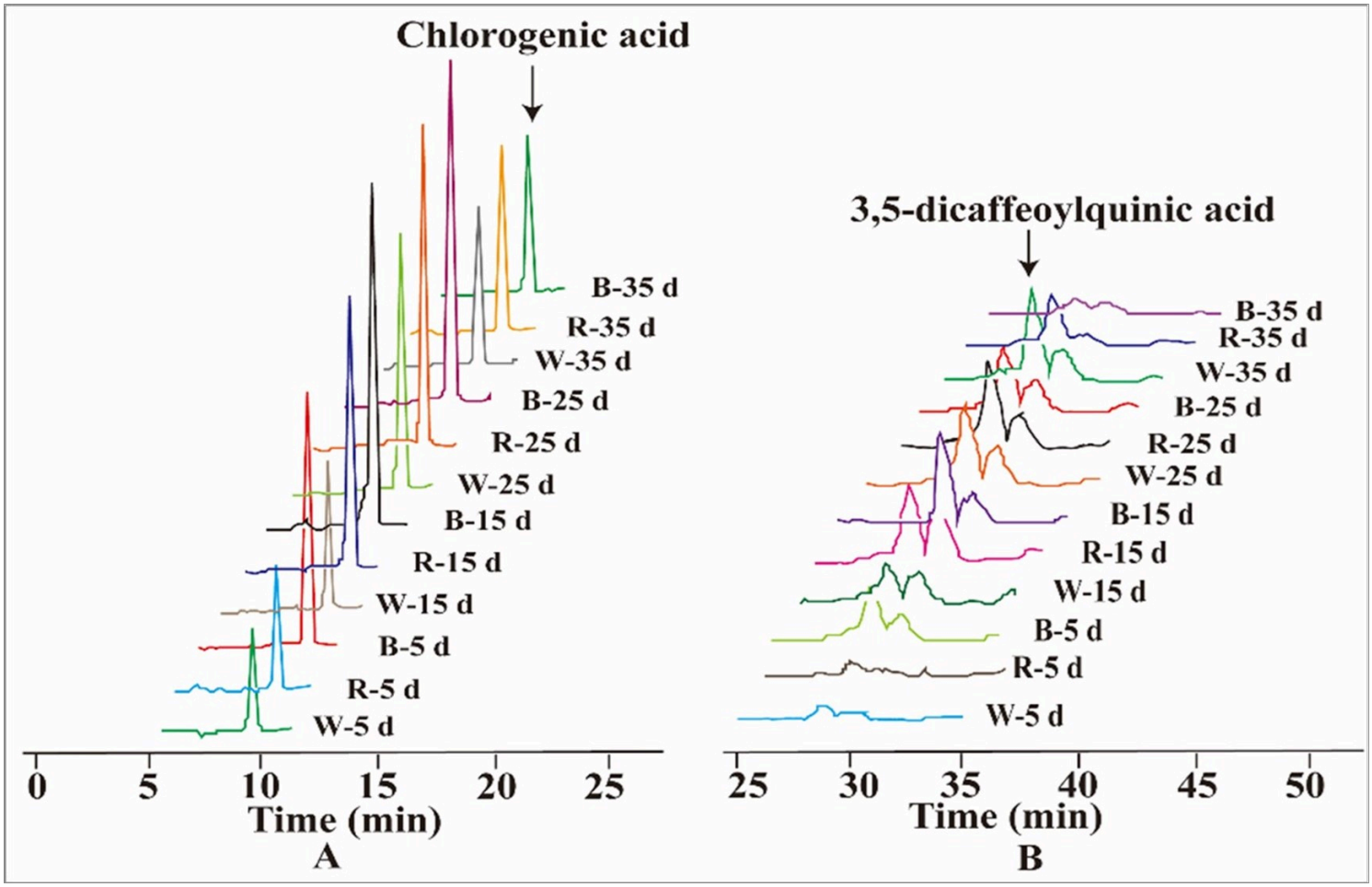


Figure 7

HPLC chromatogram of chlorogenic acid and 3,5-dicaffeoylquinic acid A

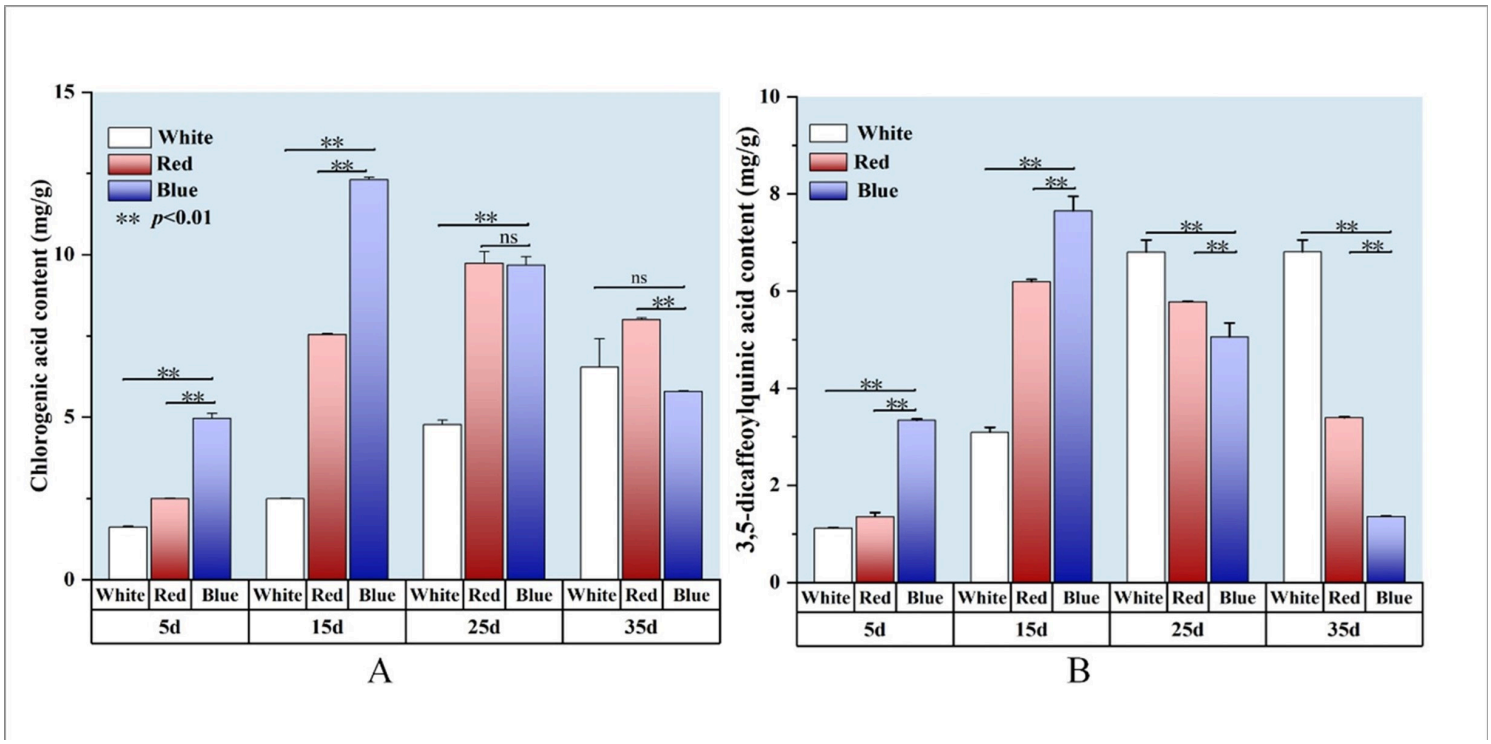


Figure 8

Effects of different light qualities on the chlorogenic acid and 3,5-dicaffeoylquinic acid content in *L. japonica* callus. Calli were harvested at 5, 15, 25, and 35 d. ** represents extremely significant differences compared with blue light at the 0.01 level ($p < 0.01$) by Duncan's new multiple range test, ns stands for no significant difference ($p>0.05$).

Supplementary Files

This is a list of supplementary files associated with this preprint. Click to download.

- SupportingInformation.docx